BNL-69469

JOURNAL OF GEOPHYSICAL RESEARCH, VOL. 107, NO. D8, 10.1029/2001JD000896, 2002

# Comparisons of box model calculations and measurements of formaldehyde from the 1997 North Atlantic Regional Experiment

G. J. Frost,[1,2] A. Fried,[3] Y.-N. Lee,[4] B. Wert,[3,5] B. Henry,[3] J. R. Drummond,[6] M. J. Evans,[7,8] F. C. Fehsenfeld,[1] P. D. Goldan,[1] J. S. Holloway,[1,2] G. Hübler,[1,2] R. Jakoubek,[1] B. T. Jobson,[1,2,9] K. Knapp,[1,2,10] W. C. Kuster,[1] J. Roberts,[1] J. Rudolph,[11] T. B. Ryerson,[1] A. Stohl,[12] C. Stroud,[1,2,5,13] D. T. Sueper,[1,2] M. Trainer,[1] and J. Williams[1,2,14]

Received 31 May 2001; revised 16 October 2001; accepted 16 November 2001; published 18 April 2002.

[1] Formaldehyde ($CH_2O$) measurements from two independent instruments are compared with photochemical box model calculations. The measurements were made on the National Oceanic and Atmospheric Administration P-3 aircraft as part of the 1997 North Atlantic Regional Experiment (NARE 97). The data set considered here consists of air masses sampled between 0 and 8 km over the North Atlantic Ocean which do not show recent influence from emissions or transport. These air masses therefore should be in photochemical steady state with respect to $CH_2O$ when constrained by the other P-3 measurements, and methane oxidation was expected to be the predominant source of $CH_2O$ in these air masses. For this data set both instruments measured identical $CH_2O$ concentrations to within 40 parts per trillion by volume (pptv) on average over the 0–800 pptv range, although differences larger than the combined $2\sigma$ total uncertainty estimates were observed between the two instruments in 11% of the data. Both instruments produced higher $CH_2O$ concentrations than the model in more than 90% of this data set, with a median measured-modeled [$CH_2O$] difference of 0.13 or 0.18 ppbv (depending on the instrument), or about a factor of 2. Such large differences cannot be accounted for by varying model input parameters within their respective uncertainty ranges. After examining the possible reasons for the model-measurement discrepancy, we conclude that there are probably one or more additional unknown sources of $CH_2O$ in the North Atlantic troposphere. *INDEX TERMS:* 0365 Atmospheric Composition and Structure: Troposphere—composition and chemistry; 0345 Atmospheric Composition and Structure: Pollution—urban and regional (0305); *KEYWORDS:* formaldehyde, photochemical modeling, aircraft measurements, North Atlantic troposphere

## 1. Introduction

[2] Formaldehyde is an important photochemical product arising from the oxidation of methane ($CH_4$) and most nonmethane hydrocarbons (NMHCs). In the remote troposphere away from continental source regions, NMHCs are in low abundance, so $CH_2O$ is thought to be produced mainly from $CH_4$ oxidation by OH, as shown schematically in Figure 1. The actual path of the carbon from $CH_4$ to $CH_2O$ depends primarily on the level of nitric oxide, NO, which controls the branching between the two main fates of methyl peroxyl radical, $CH_3O_2$: reactions with $HO_2$ and with NO (Figure 1). The lower the level of NO, the more carbon at least temporarily resides in methyl hydroperoxide, $CH_3OOH$, before going on to produce $CH_2O$. $CH_3OOH$ can be deposited to land and ocean surfaces and, to a lesser extent, to cloud droplets, removing the carbon from the system before formaldehyde can be formed. Self-reactions of $CH_3O_2$ represent only a minor branch in methane oxidation. As demonstrated in Figure 1, all carbon in the methane oxidation cycle which is not heterogeneously removed eventually proceeds through $CH_2O$ before going on to CO and $CO_2$. Measurement of $CH_2O$ along with its precursor compounds thus provides an important check on the chemical mechanism.

[3] *Fried et al.* [2002] give an extensive review of previous measurements and model calculations of $CH_2O$ in the remote

[1]Aeronomy Laboratory, National Oceanic and Atmospheric Administration, Boulder, Colorado, USA.
[2]Cooperative Institute for Research in Environmental Sciences, University of Colorado, Boulder, Colorado, USA.
[3]Atmospheric Chemistry Division, National Center for Atmospheric Research, Boulder, Colorado, USA.
[4]Environmental Chemistry Division, Brookhaven National Laboratory, Upton, New York, USA.
[5]Department of Chemistry, University of Colorado, Boulder, Colorado, USA.
[6]Department of Physics, University of Toronto, Toronto, Ontario, Canada.
[7]Centre for Atmospheric Science, Department of Chemistry, Cambridge University, Cambridge, UK.
[8]Now at Department of Earth and Planetary Sciences, Harvard University, Cambridge, Massachusetts, USA.
[9]Now at Battelle Pacific Northwest National Laboratory, Richland, Washington, USA.
[10]Now at Department of Chemistry, Pennsylvania State University, York Campus, York, Pennsylvania, USA.
[11]Centre for Atmospheric Chemistry, Department of Chemistry, York University, York, Ontario, Canada.
[12]Lehrstuhl für Bioklimatologie und Immissionsforschung, Technische Universität München, Freising-Weihenstephan, Germany.
[13]Now at Atmospheric Chemistry Division, National Center for Atmospheric Research, Boulder, Colorado, USA.
[14]Now at Abteilung Chemie der Atmosphare, Max Planck Institut für Chemie, Mainz, Germany.


0148-0227/02/2001JD000896$09.00

Research by BNL investigators was performed under the auspices of the U.S. Department of Energy under Contract No. DE-AC02-98CH10886.

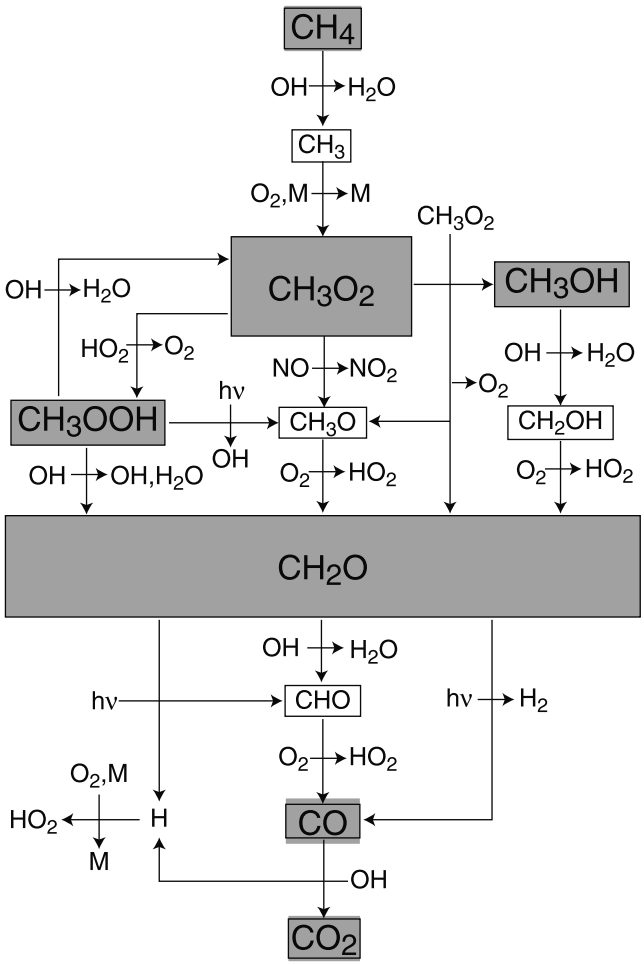


**Figure 1.** Schematic representation of the methane oxidation cycle with carbon-containing species shown in boxes. The shaded boxes indicate those species with tropospheric lifetimes longer than 1 s when [NO] <1 ppbv. Only photochemical reactions are shown; surface emission and physical removal processes are not included.

troposphere. Measurements of $CH_2O$ in relatively unpolluted marine regions are quite variable [*Zafiriou et al.*, 1980; *Lowe and Schmidt*, 1983; *Arlander et al.*, 1990; *Heikes*, 1992; *Harris et al.*, 1992; *Arlander et al.*, 1995; *Heikes et al.*, 1996; *Zhou et al.*, 1996; *Mackay et al.*, 1996; *Jacob et al.*, 1996; *Ayers et al.*, 1997; *Jaeglé et al.*, 2000; *Weller et al.*, 2000]. However, most of the studies have found $CH_2O$ mixing ratios of greater than 0.1 ppbv within the marine boundary layer, with generally higher levels for warmer or wetter locations. [$CH_2O$] is observed to decrease at higher altitudes [*Arlander et al.*, 1995; *Jacob et al.*, 1996; *Jaeglé et al.*, 2000]. These measurements have been compared to calculations ranging from simple steady state expressions [*Arlander et al.*, 1995; *Zhou et al.*, 1996] to box models [*Liu et al.*, 1992; *Jacob et al.*, 1996; *Ayers et al.*, 1997; *Jaeglé et al.*, 2000; *Weller et al.*, 2000] to two-dimensional (2-D) [*Lowe and Schmidt*, 1983; *Arlander et al.*, 1995] and 3-D models [*Brasseur et al.*, 1996]. The models in some cases show good agreement with the observations, but discrepancies in both directions and as large as a factor of 2 or more are also seen.

[4] There are a number of reasons why models can fail to capture the observed levels of $CH_2O$ accurately. Even the steady state expressions mentioned above are actually quite complicated, since they require input ([OH], for example) from some other model which in these cases was run for conditions not identical to those of the $CH_2O$ measurements themselves [*Arlander et al.*, 1995; *Zhou et al.*, 1996]. The important role of $CH_3OOH$ as a secondary source of $CH_2O$ has been noted in a number of these studies. Some differences between modeled and measured [$CH_2O$] result from whether [$CH_3OOH$] is constrained to measurements or calculated, and if calculated, whether deposition of $CH_3OOH$ is taken into account [*Liu et al.*, 1992; *Zhou et al.*, 1996; *Brasseur et al.*, 1996]. Some studies [*Arlander et al.*, 1995; *Weller et al.*, 2000] use model underestimates to suggest that methane oxidation alone does not provide a strong enough source of $CH_2O$ and that NMHCs may play an important role in formaldehyde production in the background troposphere. Others [*Lowe and Schmidt*, 1983; *Zhou et al.*, 1996] see good agreement of measurements with a methane-only model in at least some cases. Still others find model overestimates of the observations [*Jacob et al.*, 1996; *Zhou et al.*, 1996] even if [$CH_3OOH$] is constrained to measurements and surface deposition of $CH_2O$ is included. Most of the above studies do not make any explicit selection of the data to eliminate polluted air masses, relying on the relative isolation of the measurement site to provide a bias toward cleaner air. Some recent $CH_2O$ model-measurement comparisons [*Ayers et al.*, 1997; *Jaeglé et al.*, 2000] find model underestimates even if measured levels of known volatile organic compound (VOC) precursors of $CH_2O$ are included in the model. The discrepancies seen by *Jaeglé et al.* [2000] are particularly disturbing since observations of [OH] were also available, allowing the known $CH_2O$ source terms to be completely constrained by measurements. We note that most of the above comparisons cannot draw upon extensive $CH_2O$ measurements from two independent techniques.

[5] This is the second of two papers examining formaldehyde ($CH_2O$) measurements in the North Atlantic troposphere. The previous paper [*Fried et al.*, 2002] discussed a thorough comparison of $CH_2O$ measurements made by two independent instruments on the National Oceanic and Atmospheric Administration (NOAA) P-3 aircraft and presented $CH_2O$ distributions during the 1997 North Atlantic Regional Experiment (NARE 97). That paper also examined in detail numerous aspects related to $CH_2O$ measurement accuracy. For the entire NARE 97 5-min resolution data set the $CH_2O$ measurements agreed to better than 80 parts per trillion by volume (pptv) over the 0–800 pptv concentration range, though with larger scatter than can be accounted for by the known uncertainties in the two techniques. The present paper compares box model calculations with these measurements for a subset of the data where photochemical steady state can be expected. The comparisons of the $CH_2O$ measurements made by *Fried et al.* [2002] and in the present paper (section 3.2) indicate that the measurements provide a reliable database for model comparisons. The purpose of the present paper is to evaluate a photochemical box model's ability to predict $CH_2O$ in the background North Atlantic troposphere. The model uses as input simultaneously measured $CH_3OOH$ and NMHCs along with observations of methane and some oxygenated VOCs taken from other studies. Radical species such as OH are calculated self-consistently with $CH_2O$. All calculations are carried out for the measured humidity and temperature, and air masses are screened for any influence from recent pollution. This study should provide a reasonable check of whether or not methane oxidation alone is sufficient to explain the observed $CH_2O$ distributions.

## 2. Methods

### 2.1. Measurements

[6] Two instruments onboard the NOAA P-3 simultaneously measured formaldehyde during eight flights. The National Center for Atmospheric Research (NCAR) $CH_2O$ instrument consisted of a tunable diode laser absorption spectrometer (TDLAS) coupled to a multipass Herriott cell providing 100 m total optical path length.

The Brookhaven National Laboratory (BNL) instrument used the coil/2,4-dinitrophenylhydrazine (CDNPH) technique. In the NARE 97 implementation of CDNPH, samples of ambient gas phase $CH_2O$ were collected into a glass coil containing an aqueous solution of the DNPH derivatizing reagent. The liquid samples were stored sequentially in sealed glass vials using an autosampler. The DNPH-$CH_2O$ derivative in the liquid samples was then analyzed on the ground after the flight using a high-performance liquid chromatograph (HPLC) equipped with a UV-visible detector. A more detailed description of the two $CH_2O$ instruments and an intercomparison of their data for NARE 97 are given by *Fried et al.* [2002]. The two instruments were operated completely independently and used different measurement principles, sample inlets, and calibration standards and procedures. Final data were prepared by each set of $CH_2O$ investigators without communication with the other measurement group.

[7] Beside the formaldehyde measurements, other observations were made on board the P-3 during NARE 97 which were relevant to the modeling work described here. These measurements included altitude, pressure, temperature, relative humidity, water vapor mixing ratio, wind speed and direction, and the mixing ratios of $O_3$, NO, $NO_y$, peroxy acetyl nitrate (PAN), peroxy propionyl nitrate (PPN), $H_2O_2$, $CH_3OOH$, CO, and NMHCs including $C_2$–$C_6$ alkanes, $C_2$–$C_4$ alkenes, $C_2$–$C_4$ alkynes, and isoprene. Table 1 lists the median, average, and standard deviation of selected measurements in three altitude ranges for the reduced NARE 97 data set described in section 2.3.

[8] The solar near-ultraviolet irradiance was measured by two Eppley radiometers mounted in zenith and nadir orientations on the P-3. However, the zenith radiometer was damaged just before the first flight of NARE 97, and its signal was significantly lower than expected. Rather than attempt to correct the measured zenith irradiances (which were usually the larger contribution to the total irradiance) and try to derive photolysis rate coefficients ($j$ values) from these data, we instead chose to rely upon a radiative transfer model to provide $j$ values. A description of this model is given in section 2.2, and tests of the chemical model's sensitivity to the calculated $j$ values are described in section 3.3.

### 2.2. Model Description

[9] The basic modeling approach was to calculate steady state [$CH_2O$] simultaneously with the steady state concentrations of a number of other short-lived compounds at each point with available measured input data, which were held fixed in the calculations. The details of this approach are given in this section.

[10] The box model employed the same chemical mechanism as *Frost et al.* [1998]. This scheme included explicit oxidation mechanisms of alkanes with up to four carbon atoms, ethene, propene, toluene, isoprene, and $\alpha$-pinene. Other NMHCs were lumped together with one of the above species by weighting their concentrations by their OH reaction rates. Rate constants were the latest Jet Propulsion Laboratory (JPL) recommendations [*DeMore et al.*, 1997], or when not available there, were obtained from *Atkinson* [1994]. No physical processes, such as dry and wet deposition or surface emission, were included in the model. For the data set used here (see section 2.3), such processes are expected to be of minor importance relative to purely chemical terms. Evidence confirming this expectation is given below.

[11] Photolysis rate coefficients were calculated off-line by the Madronich TUV model (S. Madronich et al., Tropospheric ultraviolet-visible radiation model, Version 3.8, available at http://www.acd.ucar.edu/TUV/, 1997) using a pseudospherical discrete ordinates solution of the radiative transfer equation [*Dahlback and Stamnes*, 1991]. Cross sections and quantum yields were from *DeMore et al.* [1997]. Vertical profiles of temperature, pressure, and $O_3$ were taken from the *U.S. Standard Atmosphere* [1976]. The $O_3$ profile was scaled to give a surface overhead column of 302 Dobson units (DU), the average for the NARE 97 period and P-3 flight region according to the Total Ozone Mapping Spectrometer (TOMS) (range for NARE 97 was 283–332 DU). Surface albedo was assumed to be 5%. Aerosol optical depths from *Elterman* [1968] were assumed to be representative of background conditions. No clouds were included in the model. For the box model runs, $j$ values were interpolated for the appropriate zenith angle and altitude from the table of values generated by TUV and used without further adjustment.

[12] The box model was run in diurnal mode, meaning the zenith angles and corresponding $j$ values were varied through consecutive diurnal cycles. All calculations were run to diurnal steady state, i.e., until consecutive cycles in all calculated species were constant. All parameters measured on the P-3, besides the $CH_2O$ and NO mixing ratios, were held constant throughout the simulations; these fixed compounds included $H_2O$, $O_3$, $NO_y$, $H_2O_2$, $CH_3OOH$, CO, NMHCs, PAN, and PPN. Measured NO was used to calculate the steady state $NO_2$ at the starting point of the model run. The resulting $NO_x = NO + NO_2$ was then held fixed throughout the rest of the calculation, while NO and $NO_2$ were allowed to vary through complete diurnal cycles (though always constrained to be in steady state with one another). A few potentially important compounds were not measured on the P-3, so their concentrations were either assumed or taken from other field missions and were held fixed in the calculations. [$CH_4$] was assumed to be 1.8 ppmv, consistent with recent measurements [*Dlugokencky et al.*, 1994]. [$H_2$] was assumed to be 0.5 ppmv. [$CH_3OH$] was assumed to be 700 pptv based on data from *Singh et al.* [1995] for northern midlatitudes. Acetone mixing ratios (Table 1) were derived from the measured CO mixing ratios using a fit to Pacific Exploratory Mission, Phase B correlations of [acetone] with [CO] [*Singh et al.*, 1995, 1997]. The concentrations of $CH_2O$, OH, $HO_2$, speciated $RO_2$, $NO_3$, $N_2O_5$, $HNO_2$, $HNO_4$, acetaldehyde, lumped higher aldehydes, lumped organic peroxides besides $CH_3OOH$, and peroxyacyl nitrates besides PAN and PPN were calculated to diurnal steady state. $HNO_3$ was taken to be the difference between measured $NO_y$ and the sum of measured and calculated reactive nitrogen species ($NO + NO_2 + NO_3 + 2N_2O_5 + HNO_2 + HNO_4$ + PAN + PPN + other peroxyacyl nitrates).

### 2.3. Data Handling

[13] The goal of this study is to compare the formaldehyde measurements to the steady state concentrations derived from the box model. The modeling scheme described above requires the data set to be chosen such that the quantities held fixed in the calculations do not vary much during the time it takes $CH_2O$ to achieve diurnal steady state. For the typical conditions encountered in NARE 97, $CH_2O$ reaches steady state after one diurnal cycle, so the fixed quantities in the calculation should not change significantly over at least one diurnal cycle. From this requirement several constraints on the data set follow: (1) the model inputs must be relatively constant throughout their averaging periods; (2) there can be no recent input of $CH_2O$ precursor compounds to the air mass; and (3) the concentrations of NMHCs and $NO_x$ must have decreased to relatively low levels (the maximum concentrations of specific compounds in the data set are described below). Our attempts to achieve these constraints are discussed further below.

[14] The NCAR $CH_2O$ data were collected for 20-s intervals every minute, while the BNL data were consecutive 5-min averages. To remove the disparity between the sampling intervals of the two measurements, improve their precision, and provide a time base for averaging inputs to the box model, we constructed a data set consisting of "constant" air mass flight legs. We selected all of the intervals of 5 min or longer during NARE 97 in which specific air mass tracers remained within given ranges. The standard deviations in equivalent potential temperature and relative humidity were required to be less than 1 K and 7%, respectively, for a leg to be considered constant. The total change in altitude throughout most such legs was less than 100 m and was not allowed to exceed

**Table 1.** Median, Average, and Standard Deviation of Selected Quantities for Various Altitude Ranges From the 86 Constant Air Mass Legs Described in This Work[a]

| | | 0–2 km | | | 2–4 km | | | 4–8 km | | |
|---|---|---|---|---|---|---|---|---|---|---|
| Quantity | Units | Medium | Average | s.d. | Medium | Average | s.d. | Medium | Average | s.d. |
| $T$ | °C | 15.1 | 14.6 | 4.8 | 3.1 | 3.1 | 4.6 | −10.3 | −10.6 | 5.0 |
| $[H_2O]$ | g kg$^{-1}$ | 9.1 | 9.0 | 3.5 | 4.0 | 3.7 | 2.3 | 1.2 | 1.5 | 1.2 |
| $[O_3]$ | ppbv | 38 | 38 | 7 | 49 | 47 | 10 | 50 | 52 | 11 |
| [NO] | pptv | 4 | 6 | 5 | 7 | 9 | 7 | 11 | 12 | 8 |
| [PAN] | pptv | 34 | 42 | 40 | 56 | 97 | 104 | 110 | 144 | 110 |
| $[NO_y]$ | pptv | 306 | 351 | 197 | 259 | 352 | 218 | 343 | 398 | 268 |
| [CO] | ppbv | 90 | 90 | 11 | 88 | 90 | 11 | 87 | 86 | 13 |
| $[C_2H_6]$ | pptv | 737 | 727 | 148 | 631 | 702 | 208 | 689 | 719 | 233 |
| $[C_3H_8]$ | pptv | 168 | 157 | 66 | 119 | 146 | 111 | 151 | 170 | 131 |
| $[n\text{-}C_4H_{10}]$ | pptv | 26 | 31 | 21 | 21 | 29 | 36 | 24 | 33 | 32 |
| $[i\text{-}C_4H_{10}]$ | pptv | 17 | 18 | 10 | 14 | 17 | 18 | 12 | 16 | 15 |
| $[CH_3OOH]$ | ppbv | 0.29 | 0.37 | 0.22 | 0.37 | 0.39 | 0.18 | 0.23 | 0.23 | 0.11 |
| [acetone] | pptv | 370 | 370 | 40 | 360 | 370 | 50 | 360 | 360 | 50 |
| NCAR $[CH_2O]$ | ppbv | 0.39 | 0.41 | 0.11 | 0.29 | 0.29 | 0.12 | 0.22 | 0.25 | 0.11 |
| BNL $[CH_2O]$ | ppbv | 0.36 | 0.42 | 0.15 | 0.36 | 0.37 | 0.15 | 0.26 | 0.27 | 0.13 |
| Model $[CH_2O]$ | ppbv | 0.25 | 0.25 | 0.07 | 0.14 | 0.17 | 0.07 | 0.10 | 0.10 | 0.03 |

[a] All quantities were measured on the NOAA P-3 during NARE 97 except model $[CH_2O]$ and [acetone], which was derived from the P-3 [CO] using a fit to Pacific Exploratory Mission, Phase B correlations of [acetone] with [CO] [*Singh et al.*, 1995, 1997]. Number of data points in each altitude range: 0–2 km = 31, 2–4 km = 27, and 4–8 km = 28.

1200 m. These limits, though somewhat arbitrary, provided conservative constraints to ensure that conditions remained constant throughout the legs.

[15] All measured chemical concentrations and physical variables were then averaged over these legs. In the case of low-frequency measurements such as NMHCs, multiple observations within a leg were averaged if available. Otherwise, the single sample taken during the leg was assumed to be representative of the entire leg.

[16] We assumed that all air parcels encountered within these constant legs were relatively homogeneous and had similar histories. This assumption was supported by back trajectories calculated from European Centre for Medium-Range Weather Forecasts (ECMWF) analyses [*ECMWF*, 1995] using the code of *Methven* [1997]. Three-dimensional back trajectories were calculated along the flight track for all the NARE flights and were distributed via a web site (M. J. Evans, Centre for Atmospheric Science, University of Cambridge, Cambridge, UK, Cambridge Trajectory Server, available at http://www.atm.ch.cam.ac.uk/~mathew/trajectories/start.html, 1998). These back trajectories showed that all of the air masses encountered during a given constant leg had a common origin both vertically and horizontally within 3 days before sampling for more than 80% of the legs and within 2 days for more than 95% of them. Realizing that trajectory calculations have

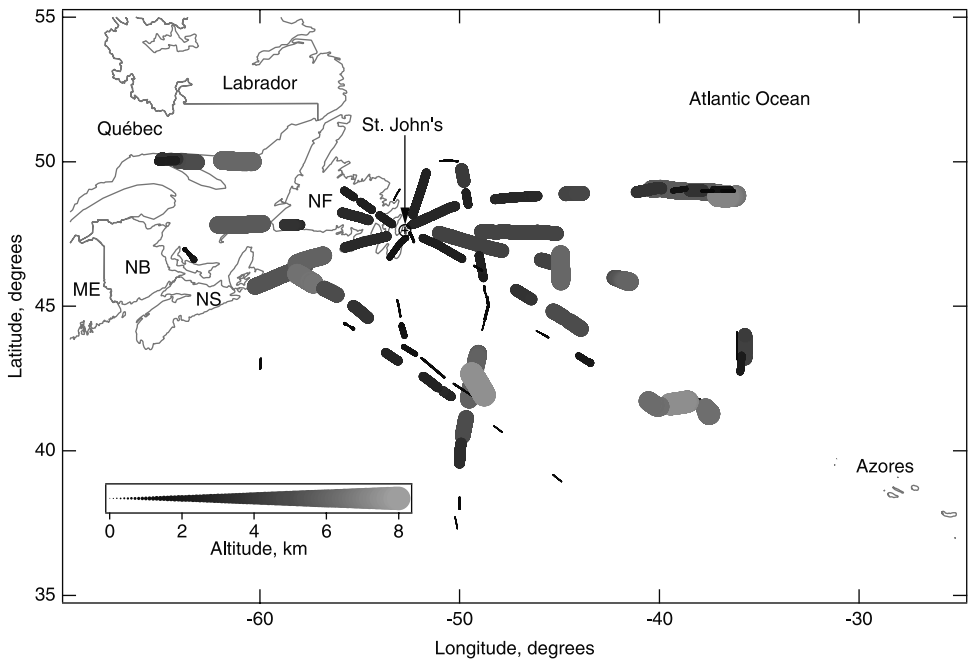


**Figure 2.** Map showing the location, length, and altitude of the 86 constant air mass flight legs described in the text. The altitude of each leg is indicated both by the shading and size of the marker. NF, Island of Newfoundland; NB, New Brunswick; NS, Nova Scotia; ME, Maine.

several inherent error sources, we did not eliminate a leg if the trajectories showed influences of air masses with different histories.

[17] Emissions of $NO_x$ and NMHCs from anthropogenic, biogenic, or lightning sources to the air masses could also perturb $CH_2O$ levels if these emissions occurred within a few days of the measurement period. Constraining the input of the model to the measured values of these compounds would underestimate their initial levels if they were changing rapidly, as would be the case within a few days of emission. The model would therefore underestimate the amount of $CH_2O$ produced if an air mass had recently been influenced by emissions. We addressed this problem in several ways. First, any air mass legs with large variations in the concentrations of $O_3$, CO, or $NO_y$ were omitted: within any leg, standard deviations were less than 8, 8, and 0.3 ppbv for $O_3$, CO, and $NO_y$, respectively, while the relative standard deviations in these compounds averaged 3, 4, and 12%, respectively. This step removed some legs which contained recently emitted pollution plumes. We also used an air mass age analysis to pinpoint air masses with recent anthropogenic $NO_x$ emissions. This analysis used the FLEXPART particle dispersion model [*Stohl et al.*, 1998] with ECMWF wind fields of similar spatial resolution ($0.5° \times 0.5°$ within the NARE region, $1° \times 1°$ outside) and higher time resolution (3 hours) as those used to calculate the Evans (Cambridge Trajectory Server, 1998) back trajectories. Details of the FLEXPART model runs for NARE 96 and 97 are described by *Stohl et al.* [2002]. Using the FLEXPART model, the levels of a passive tracer emitted as $NO_y$ from North America in each air mass were tabulated as a function of time since emission. On the basis of this analysis we eliminated several legs which either (1) contained at least 1 ppbv $NO_y$ and were emitted less than 2 days before the measurement point, or (2) contained at least 5 ppbv $NO_y$ and were emitted within 6 days prior to measurement. Finally, two other legs with elevated levels of NO which were not caught by the FLEXPART analysis were also eliminated.

[18] After the above restrictions were imposed, there were 86 constant air mass flight legs (5–51 min duration) remaining which contained data from both $CH_2O$ instruments and with sufficient input to make a model calculation. The location, length, and altitude of these legs are shown in Figure 2. The resulting data set had relatively low levels of nitrogen oxides and NMHCs, as shown in Table 1. For this data set the maximum mixing ratios of NO, $NO_y$, CO, *n*-butane, and isoprene were 44 pptv, 1.2 ppbv, 127 ppbv, 175 pptv, and 36 pptv, respectively. The mixing ratios of other measured NMHCs ($C_5$-$C_6$ alkanes, ethene, propene, and isoprene) were at or below their detection limits in most of the legs. The measurements in this data set were made in September 1997 in the region from 37° to 50°N latitude and from 35° to 65°W longitude between the surface and 8 km altitude.

## 3. Results and Discussion

### 3.1. $CH_2O$ and $CH_3O_2$ Sources and Sinks

[19] The data set considered here consists of relatively clean air masses, as demonstrated by the median, diurnally averaged sources of formaldehyde (Figure 3). The largest source of $CH_2O$ is the reaction of $CH_3O_2$ with NO. Smaller sources include self-reaction of $CH_3O_2$ and reactions involving $CH_3OOH$, itself a product of $CH_3O_2$ reaction with $HO_2$ (Figure 1). Thus the predominant sources of $CH_2O$ are all reactions of $CH_3O_2$ or its products. The main source of $CH_3O_2$ is the direct oxidation of methane by OH. Direct or secondary production of $CH_2O$ or $CH_3O_2$ from NMHCs is minor. Taking into account the levels of the known $CH_2O$ precursors in these air masses, the model predicts nearly all of the measured $CH_2O$ should arise from methane oxidation.

[20] The model-derived $CH_2O$ diurnally averaged loss rates indicate a median photochemical lifetime of 7 hours for the conditions of this data set. All of the known tropospheric photochemical $CH_2O$ sinks, the two photolysis channels and OH reaction, contribute significantly to the $CH_2O$ lifetime. Light influences both the production and loss of $CH_2O$ since photolysis is a direct sink but other photolysis reactions provide the source species. As a result, we do not expect steady state $CH_2O$ to be very sensitive to overall changes in light intensity, although light will influence the time required to achieve diurnal steady state. On the other hand, NO is important in determining $CH_2O$ levels because it controls the branching between the direct production of $CH_2O$ by $CH_3O_2$ + NO and the diversion of $CH_3O_2$ to peroxide formation by reaction with $HO_2$ (Figure 1). Hence, if we choose to fix $NO_x$ levels in our calculations, we need to select air masses where $NO_x$ levels are changing very slowly, which is the case when [NO] <50 pptv.

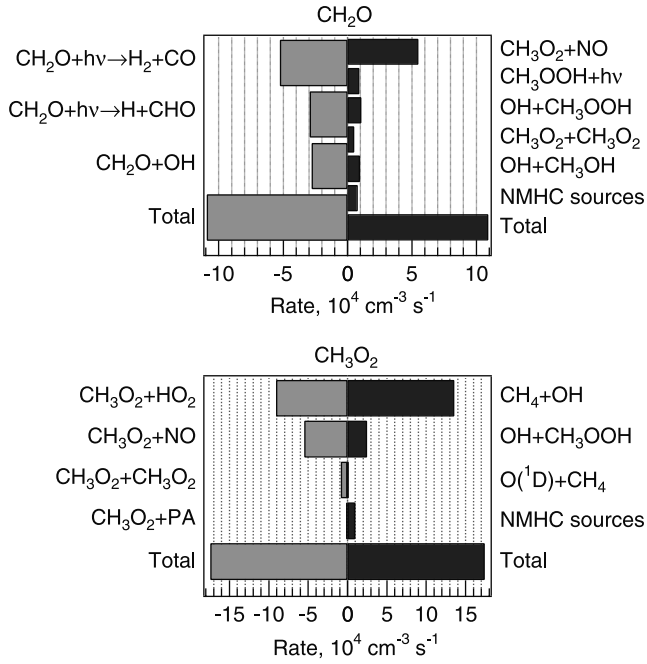


**Figure 3.** Diurnally averaged (left half of each panel) loss and (right half of each panel) production rates for (top) $CH_2O$ and (bottom) $CH_3O_2$ calculated by the box model. Median values are shown for the data set of 86 points discussed in this work. PA, peroxy acetyl radical.

### 3.2. $CH_2O$ Model-Measurement Comparisons

[21] Scatterplots comparing modeled and measured [$CH_2O$] are shown in Figure 4, and distributions of the differences are presented in Figure 5. Tables 2 and 3 give the statistics derived from these comparisons. The correlation coefficients ($r^2$) between the model and either instrument and between the two instruments are fairly low: $r^2 = 0.26$ between the two instruments, and $r^2 \approx 0.35$ between the model and either instrument. Despite the low correlation coefficient, the slope of the bivariate weighted fit to a scatterplot of the two instruments' data is 1 to within the error of the fit ($1.04 \pm 0.19$). In contrast, the slope of a similar fit to either instrument's data plotted against the model is significantly different from 1, and the slopes of the two measurement-model fits agree with each other to within the uncertainties. All of these fits have *y* intercepts which are not statistically different from zero. From the $CH_2O$ mixing ratio difference distributions we find that the average and median differences between the instruments are only 0.04 and 0.02 ppbv, respectively. However, the spread in the instrument difference distribution is wide, reflecting low correlation between the two techniques. Significant differences between the instruments larger than the combined $2\sigma$ total uncertainty estimates (estimated

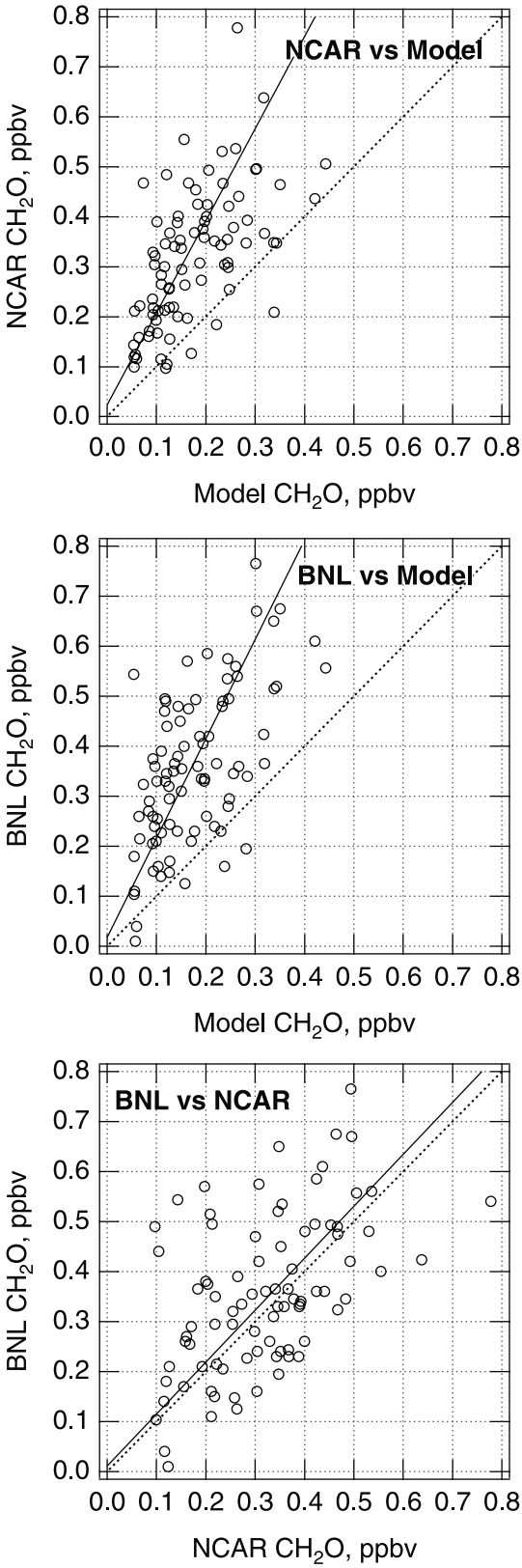


**Figure 4.** Measured and modeled [$CH_2O$] comparison scatterplots, showing the 86 data points (circles), the weighted least squares bivariate fit (solid line), and the 1:1 line (dotted line).

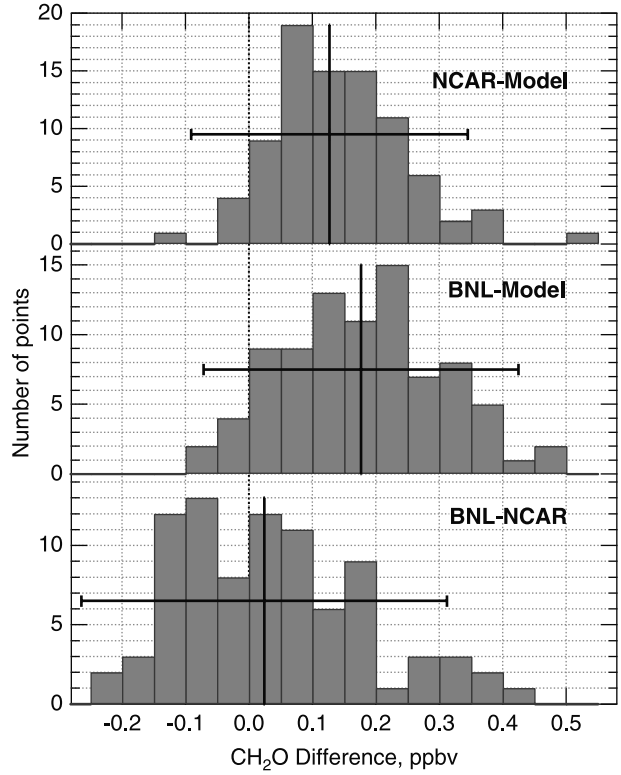


**Figure 5.** Distribution of absolute differences between measured and modeled [$CH_2O$] for the full data set of 86 points. The solid black vertical lines are the median differences, and the horizontal bars indicate 2 standard deviations.

as described in section 3.3) were observed in 11% of the data set. The measurement-model difference distributions, though also wide, both show the measurements are higher than the model, with median differences of 0.13 ppbv for the NCAR instrument and 0.18 ppbv for the BNL observations. Compared with the median modeled [$CH_2O$] of 0.15 ppbv for the entire 86-point data set, this difference is about a factor of 2. Both the scatterplots and difference distributions show that the BNL instrument measures somewhat higher $CH_2O$ mixing ratios than the NCAR instrument in general. The median difference does not differ from zero within 2 standard deviations for any of the distributions. However, the

**Table 2.** Statistics From Linear Fits of [$CH_2O$] Comparisons

| $y$ | $x$ | $r^{2a}$ | $\chi^{2b}$ | Slope ± Standard Error[b] | $y$ Intercept ± Standard Error,[b] ppbv |
|---|---|---|---|---|---|
| NCAR | model | 0.34 | 88 | 1.84 ± 0.34 | 0.02 ± 0.04 |
| BNL | model | 0.36 | 80 | 1.99 ± 0.39 | 0.02 ± 0.05 |
| BNL | NCAR | 0.26 | 84 | 1.04 ± 0.19 | 0.01 ± 0.05 |

[a] From unweighted fit.

[b] From weighted bivariate fits with weights ($f$*1σ total uncertainty)$^{-2}$, where $f$ = 0.475 for the model and $f$ = 1.35 for the NCAR and BNL measurements. In other words, the 1σ total uncertainty for each instrument needed to give the best fit between the two instruments was 35% larger than that derived initially by the instrument operators, while the best fits between modeled and measured [$CH_2O$] suggested a 1σ model uncertainty about 48% of that calculated by the uncertainty analysis in section 3.3. The measured and modeled data in the fits were initially weighted by the inverse square of their estimated 1σ total uncertainties, i.e., $f$ = 1. We then adjusted $f$ in order to obtain a best fit of $\chi^2 \approx N - 2$, where $N$ is the number of data points equal to 86, and assumed that the values of $f$ for both instruments were equal.

**Table 3.** Statistics From Distributions of $CH_2O$ Mixing Ratio Differences

| [$CH_2O$] Difference | *N* | Average, ppbv | Median, ppbv | Standard Deviation, ppbv |
|---|---|---|---|---|
| NCAR-model | 86 | 0.14 | 0.13 | 0.11 |
| BNL-model | 86 | 0.18 | 0.18 | 0.12 |
| BNL-NCAR | 86 | 0.04 | 0.02 | 0.14 |
| NCAR-model | 56[a] | 0.12 | 0.11 | 0.11 |
| BNL-model | 56[a] | 0.17 | 0.15 | 0.13 |
| BNL-NCAR | 56[a] | 0.04 | 0.02 | 0.15 |

[a] Excluding points above 2 km with elevated water vapor mixing ratios.

scatterplots and difference distributions show that the measurement-model difference is systematic, and for over 90% of the data points the measured $CH_2O$ mixing ratio (from either instrument) is larger than the model value.

[22] The data were also considered as a function of altitude and grouped into 0–2, 2–4, and 4–8 km bins (Table 1). Figure 6 shows all the [$CH_2O$] data, the $CH_2O$ mixing ratio differences, and the median values of each of these quantities for the three altitude bins. The two instruments and the model all show decreasing [$CH_2O$] with altitude. Two effects act to decrease the production rate of $CH_2O$ with increasing altitude: (1) lower water vapor concentrations result in lower OH concentrations aloft, and (2) lower temperatures decrease the rate constant of OH with $CH_4$. Figure 6 and Table 1 demonstrate that the median 0.13–0.18 ppbv difference between the model and measurements is relatively constant in the altitude range 0–8 km; for a given difference distribution the medians in each altitude bin do not differ from each other to within 1 standard deviation. The median differences between the two [$CH_2O$] measurements in each altitude bin are smaller than the median differences between the model and either measurement, but none of the median differences differs from zero within 2 standard deviations in any of these altitude bins.

[23] The model did not include surface deposition of $CH_2O$, which would decrease the calculated [$CH_2O$] in the lowest altitude bin even further. We reran the model including an additional $CH_2O$ loss term of $4 \times 10^{-6}$ $s^{-1}$ to simulate a deposition velocity of 0.4 cm $s^{-1}$ to the ocean [*Thompson and Zafiriou*, 1983]. The median modeled [$CH_2O$] in the 0–2 km bin decreases by only 0.02 ppbv if surface deposition at this rate is included. There are few direct studies of $CH_2O$ surface uptake rates [*Thompson and Zafiriou*, 1983; *Zafiriou et al.*, 1980], and *Thompson and Zafiriou* [1983] indicate that their 0.4 cm $s^{-1}$ deposition velocity estimate may be uncertain by as much as a factor of 3. A physical loss rate of $4 \pm 2 \times 10^{-6}$ $s^{-1}$ is consistent with the findings of other recent model analyses of measured $CH_2O$ distributions [*Weller et al.*, 2000; *Ayers et al.*, 1997; *Jacob et al.*, 1996; *Zhou et al.*, 1996; *Liu et al.*, 1992], although most of these studies could not distinguish between various uptake processes such as wet and dry surface deposition and uptake by fog or cloud droplets. The measured $CH_2O$ vertical profiles from NARE 97 (Figure 6) do not indicate a strong deposition loss at the lowest altitudes. Taken together, this evidence suggests that the impact of deposition on $CH_2O$ in this environment is small.

[24] The results of the comparison between the NCAR and BNL instruments discussed here are very similar to those presented in the companion paper by *Fried et al.* [2002] using both the full 5-min resolution data set and the reduced set of constant air mass legs. The reader is referred to Fried et al. for a more complete discussion of the instrument comparison. As shown above and in the work of Fried et al., although one or both instruments are less precise than originally estimated, both instruments show the same median and average values and the same altitude trends to within the uncertainties. As discussed by Fried et al., longer time averaging during constant air mass time periods produced a median difference of 7 pptv and a combined measurement precision reasonably close to that expected. The number of constant air mass legs that Fried et al. considered differed slightly from that used here, because they removed a few points in which inlet effects were thought to have influenced the BNL instrument while we did not remove these data from our analysis. As a consequence, we found somewhat lower correlation coefficients, larger absolute differ-

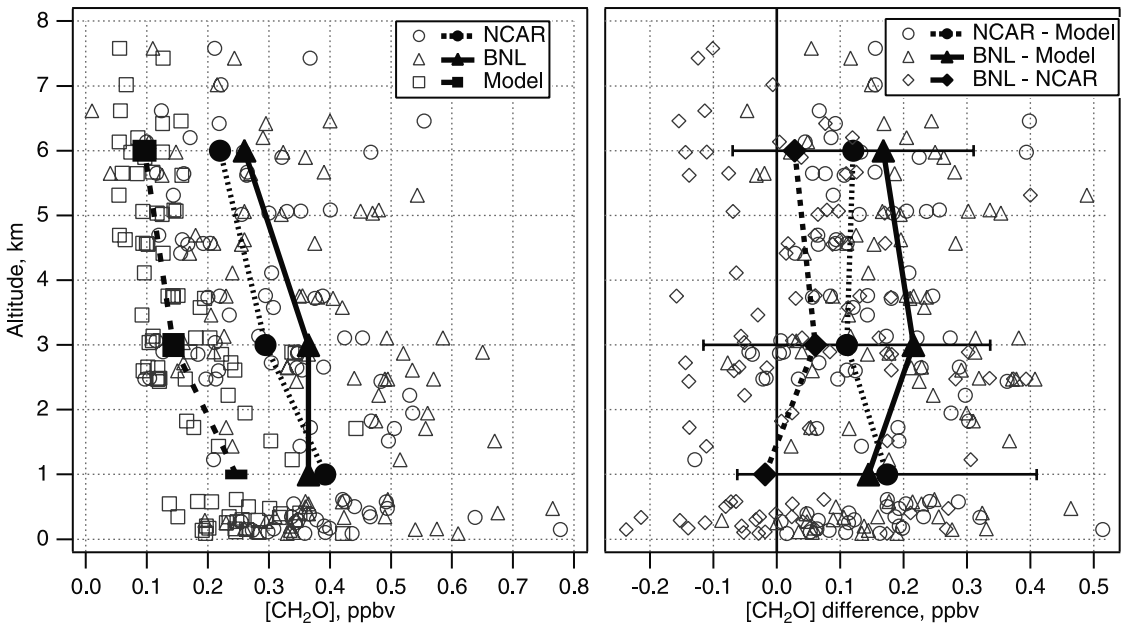


**Figure 6.** (left) $CH_2O$ mixing ratios and (right) mixing ratio differences as a function of altitude. Gray open symbols are the individual data points. Black solid symbols joined by lines are the medians for the 0–2, 2–4, and 4–8 km altitude bins. The horizontal bars in the right panel show 2 standard deviations in the NCAR-model [$CH_2O$] differences for each altitude bin. Standard deviations in the BNL-model and BNL-NCAR [$CH_2O$] differences were larger than those in the NCAR-model differences.

ences, and wider difference distributions between the two instruments than were reported by Fried et al. The robustness of these constant air mass data sets is demonstrated by the fact that despite the small differences, the conclusions drawn from them (and from the full high time-resolution data set) are the same: the two instruments, while not as well correlated as expected, on average measure the same levels of $CH_2O$. On average, these measured levels differ from the modeled levels by a greater degree than the measurements differ from one another.

### 3.3. Uncertainties and Sensitivities

[25] Uncertainties for the two instruments were derived according to the procedures described by *Fried et al.* [2002]. For both instruments, precisions (random uncertainties) were determined for each constant air mass leg, while an average uncertainty in the measurement calibrations was used for the entire mission. The 1σ precisions of the NCAR instrument ranged from ±23 to ±121 pptv, with an average of ±60 pptv, while the 1σ calibration uncertainty was found to be ±7% of the ambient mixing ratio. The BNL instrument had precisions of ±15 to ±173 pptv with an average of ±65 pptv and a calibration uncertainty of ±12% of ambient. Total uncertainty (1σ) for each instrument for each constant air mass leg was calculated by adding in quadrature the uncertainty due to precision over the leg duration and the uncertainty from calibration errors (calibration uncertainty × measured leg concentration).

[26] An estimate of the uncertainty in the model $CH_2O$ mixing ratio contributed by the input parameters was estimated using a simple sensitivity analysis approach [*McKeen et al.*, 1997]. Each input parameter (including concentrations of fixed species, rate constants, and photolysis rate coefficients) was varied by 15% up and down from its value in the base model run, and the percent difference in $[CH_2O]$ for the two extremes was calculated. The percent change in $CH_2O$ mixing ratio for the 30% change in each parameter was defined as the sensitivity to that parameter, with a positive value indicating an increase in $[CH_2O]$ when that parameter was increased. The 1σ percent uncertainty in each parameter, obtained from the literature or the instrument operators, was then multiplied by the model sensitivity, and the products for all parameters were added in quadrature. The square root of the resulting sum represents an estimate of the total 1σ model $[CH_2O]$ uncertainty. Figure 7 shows the parameters to which the model $[CH_2O]$ was most sensitive, their respective uncertainties, and their contribution to the square of the total uncertainty. The first seven parameters in Figure 7, representing the measured chemical species concentrations and the "*j* scaling factor" (a constant factor applied to all *j* values to simulate the effects of clouds), contribute randomly to the uncertainty in the model result. An error in the other 11 parameters, the rate coefficients, causes each to be systematically high or low and would therefore cause a consistent bias (whose direction is unknown) in the modeled $[CH_2O]$; we call these "systematic" uncertainties. Considering all input parameters, we derive median 1σ random, systematic, and total uncertainties of 12, 55, and 57% in the model $[CH_2O]$ from the above analysis. These values should be considered estimates since the analysis assumes that the model response will be linear when a parameter is varied through its full uncertainty range. However, this approach compares well with more exact methods [*Dunker*, 1984].

[27] The largest model sensitivities (Figure 7) were about ±0.4%/%, indicating that a 10% change in any of the input parameters caused at most only a 4% change in the calculated $[CH_2O]$. Not surprisingly, the most important sensitivities were to parameters controlling the key production and loss channels of $CH_2O$. These sensitivities were dependent on the model approach used here, which was to calculate $[CH_2O]$ simultaneously with [OH], $[HO_2]$, and $[RO_2]$. Therefore many of the parameters with high sensitivities are responsible for controlling OH levels, which in turn affect the calculated $CH_2O$ mixing ratio. Also, although

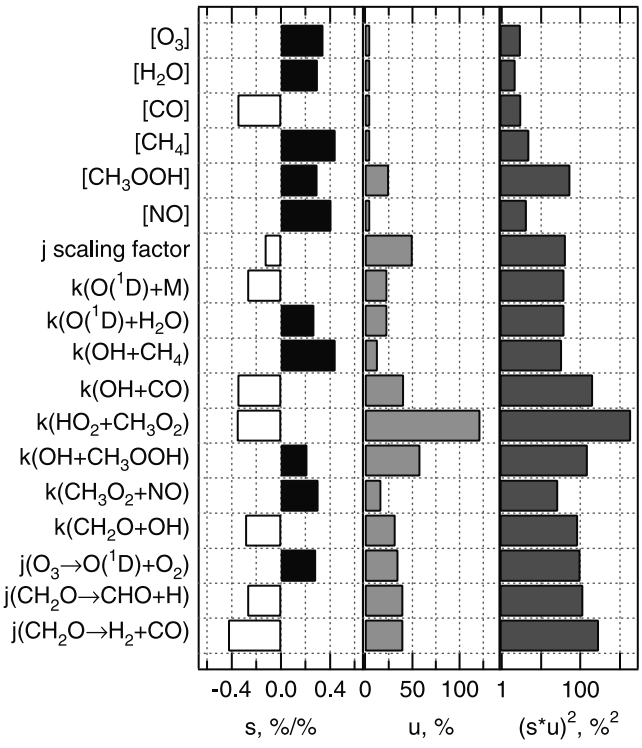


**Figure 7.** (left) Sensitivity in $[CH_2O]$ to, (middle) 1σ uncertainty in, and (right) contribution to the square of the $[CH_2O]$ uncertainty from the model input parameters, where *s* is sensitivity and *u* is uncertainty. All data are medians for the full data set of 86 points and represent the input parameters to which the modeled $[CH_2O]$ is most sensitive. The contribution of each parameter to the square of the total $[CH_2O]$ uncertainty is the square of the product of the parameter's sensitivity and uncertainty. The "*j* scaling factor" is a constant factor applied to all *j* values to simulate the effects of clouds.

model $[CH_2O]$ is sensitive to changes in individual *j* values, an equivalent change to all *j* values simultaneously (given by the *j* scaling factor in Figure 7) has a smaller effect on $[CH_2O]$. Thus the presence of clouds, which affects all *j* values approximately equally, will not drastically change the steady state concentrations of $CH_2O$, although it will change the time needed to achieve steady state. As discussed in section 3.1, $CH_2O$ sources and sinks both depend on photolysis reactions, causing $[CH_2O]$ to have a low sensitivity to a constant change in all *j* values simultaneously.

[28] While $CH_2O$ is sensitive to all of the parameters shown in Figure 7, only a few of the parameters contribute most of the uncertainty in $[CH_2O]$. The largest single source of uncertainty in the calculated $[CH_2O]$ is the rate constant for the $HO_2 + CH_3O_2$ reaction, with a 1σ uncertainty of 120% at the median temperatures of NARE 97 according to *DeMore et al.* [1997]. Other significant sources of uncertainty are the $CH_3OOH$ mixing ratio, the rate constants of OH reactions with CO, $CH_3OOH$, and $CH_2O$, and the *j* values for $O_3 \rightarrow O(^1D) + O_2$ and for the two photolysis channels of $CH_2O$.

[29] The parameters which made the largest contributions to the model $CH_2O$ uncertainty were then increased or decreased within their respective 1σ uncertainty ranges in the direction which would increase the model $[CH_2O]$ (Figure 8). Changes in the model parameters of up to a factor of 2 caused changes in $[CH_2O]$ equal to what the sensitivities in Figure 7 would predict, showing that the model response to large changes in these parameters is essentially linear. More importantly, adjusting any of these parameters within their 1σ uncertainty ranges did not increase the median model

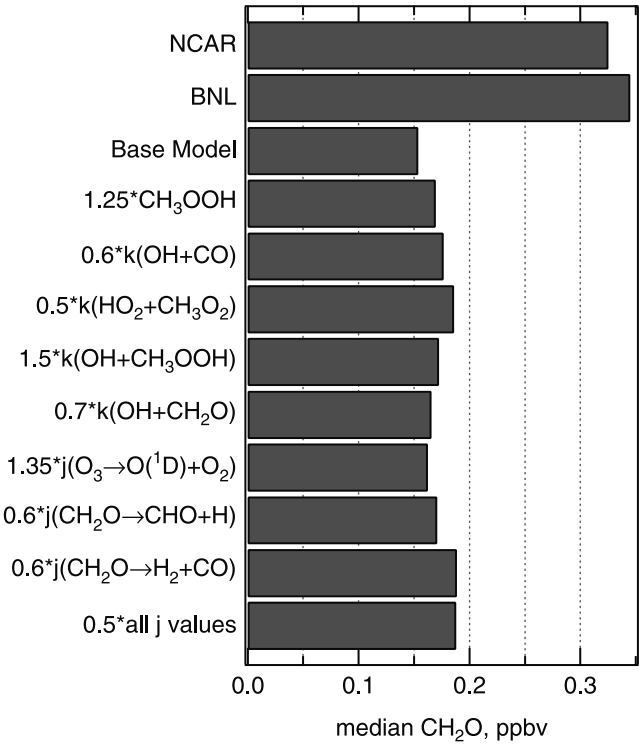


**Figure 8.** Median $CH_2O$ mixing ratios for the full data set of 86 points are shown for the two measurements, the base model, and a number of model sensitivity tests. In each test the indicated parameter was adjusted by the given amount, and the model was rerun for all points. These adjustments represent the estimated 1σ uncertainty range for the parameter and were made in the direction which would increase the modeled [$CH_2O$].

$CH_2O$ mixing ratio (0.15 ppbv) by more than 40 pptv (Figure 8). We did not carry out a sensitivity run assuming that multiple input parameters were in error, which would give a larger increase in [$CH_2O$]. However, we would need to simultaneously vary essentially all of the parameters shown in Figure 8 to their full uncertainty limits to eliminate the model-measurement [$CH_2O$] discrepancy. On the basis of this analysis the model's factor of 2 underestimate of [$CH_2O$] does not appear to result simply from inaccuracies in any single model input parameter. Much larger uncertainties than are reported for these parameters would be necessary to explain the observed discrepancies.

### 3.4. Causes and Implications of $CH_2O$ Model-Measurement Discrepancies

[30] What are the possible reasons for the factor of 2 difference between $CH_2O$ model and measurement, and can we find the most probable one? Here we discuss a number of possibilities as well as the implications of the model underestimate.

[31] A measurement problem seems the most unlikely of the possible explanations for the discrepancy because we see nearly the same results from two independent instruments. The NCAR and BNL instruments are based on completely different operating principles, each used its own sampling inlet on the P-3, and each was calibrated by a different method [*Fried et al.*, 2002]. The two instruments were compared on board the P-3 using a common standard, with agreement to within about 4%. This is not to say that instrument improvements are not needed. While the instruments agree with each other on average to within the combined uncertainties [*Fried et al.*, 2002], the point-to-point differences between them are sometimes larger than expected based on the uncertainties. The long averaging periods of the data set used here were chosen in part to reduce the scatter in the individual data points from both instruments. Improvements in the precision of each measurement would reduce the total uncertainty limits on each. Nevertheless, it is difficult to imagine how two independent measures of the $CH_2O$ mixing ratio could both be in error on average by approximately the same degree. *Fried et al.* [2002] also show that the NARE 97 [$CH_2O$] measurements are similar to other recent observations in the remote troposphere, giving us further confidence in the NARE 97 data.

[32] Our model results appear to be reasonable when compared to other calculations for similar conditions. For example, we calculate a median [$CH_2O$] of 0.25 ppbv and a range of 0.14–0.44 ppbv for the 0–2 km portion of NARE 97. Methane-only calculations for the same altitude range in the NARE region presented by *Lowe and Schmidt* [1983] and *Arlander et al.* [1995] suggest 0.12–0.25 ppbv $CH_2O$ in October and 0.1–0.2 ppbv in January, respectively. *Ayers et al.* [1997] calculate about 0.2 ppbv at the surface at 40°S in late spring/early summer. *Jaeglé et al.* [2000] calculate a median [$CH_2O$] of 29 pptv for "background" conditions at 8–12 km between mid-October and mid-November in the NARE region, while our model predicts 36 pptv $CH_2O$ for similar conditions.

[33] Assuming steady state for $CH_2O$ with respect to the fixed precursors seems valid given the $CH_2O$ photochemical lifetime of 7 hours. We were careful to limit the data set under consideration to only clean air masses, where low levels of NMHCs and NO preclude the possibility of recent emissions of pollution or biogenic compounds. The back trajectory analyses combined with tracer emissions confirm this conclusion.

[34] $CH_2O$ steady state could have been perturbed in ascending air or in air masses transported from lower latitudes when the transport occurred on the order of a few days or less before the measurement. $CH_2O$ levels are higher for lower altitudes (Figure 6) and latitudes because of higher water vapor mixing ratios and temperatures. We considered a reduced data set of 56 points, in which points above 2 km with the highest water vapor mixing ratios were excluded (Figure 9) on the assumption that these

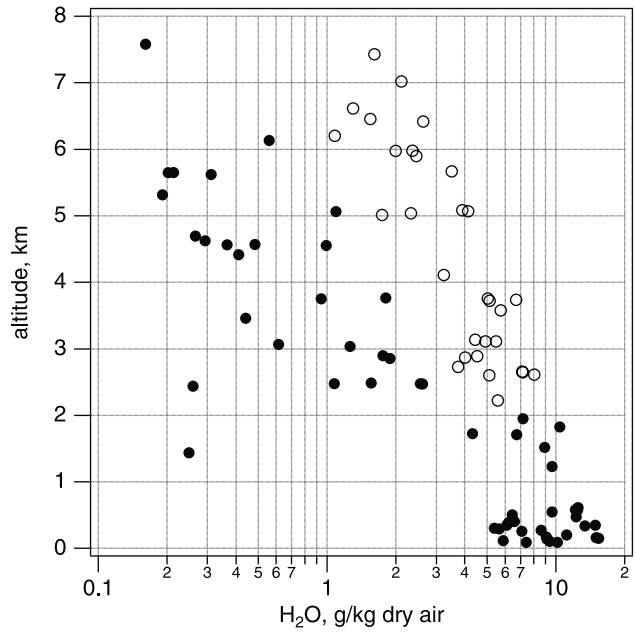


**Figure 9.** Water vapor mixing ratio as a function of altitude for the full data set of 86 points (all circles) and for a subset of 56 points in which points above 2 km with arbitrarily high [$H_2O$] were eliminated (solid circles).

elevated wet air masses may have been influenced by recent transport. We examined the back trajectories for these 30 excluded points and found that the majority provided confirmation of such transport. In 70% of these points the trajectories had, within 3 days of measurement, ascended at least 2 km or originated in the boundary layer, and/or traveled more than 10° latitude northward. Model-measurement comparisons of [$CH_2O$] for the reduced data set revealed only small differences from the full data set (Table 3). The median and average differences between the model and measurements were reduced slightly, but most of this change was due to somewhat higher model [$CH_2O$] in the reduced data set compared with the full one, which was the opposite of the expected effect of excluding the high humidity data in the free troposphere. The median and average measured $CH_2O$ mixing ratios from both instruments were nearly identical in both data sets. It appears unlikely that transport caused any systematic effect on [$CH_2O$] leading to the large measurement-model differences.

[35] The model-measurement discrepancy could be explained if $CH_2O$ sinks were much smaller than calculated. There are only three photochemical channels to consider, since including deposition or heterogeneous uptake (both neglected in the model) would only make the discrepancies worse. Varying all of the parameters controlling these channels within their 1σ uncertainty ranges did not produce more than a 25% change in the model $CH_2O$ mixing ratio (Figure 8). In addition, the median OH concentrations predicted by this model in a previous study in the remote troposphere [*Frost et al.*, 1999] were within about 30% of observations. Unless much larger uncertainties exist in either the $CH_2O$ $j$ values or $k(OH + CH_2O)$ than have been reported in the literature, there is no way to account for the $CH_2O$ model-measurement discrepancies through the sink terms.

[36] Since none of the above possibilities seems to explain the model-measurement discrepancy, it appears that the model's $CH_2O$ production rate is too small. Uncertainties in parameters controlling the known source channels do not appear large enough to explain more than a 25% discrepancy in [$CH_2O$]. We therefore postulate that at least one source of $CH_2O$ is missing from the standard model. The median missing $CH_2O$ source is about 0.4 ppbv $d^{-1}$ and is relatively constant with altitude between 0 and 8 km in the NARE 97 domain.

[37] Some possible candidates for a missing source have been mentioned in recent studies where similar model-measurement discrepancies are observed. *Ayers et al.* [1997], citing laboratory evidence, suggest that the $HO_2 + CH_3O_2$ reaction could yield up to 40% $CH_2O + H_2O + O_2$, instead of 100% $CH_3OOH + O_2$ as assumed in the standard model (Figure 1). A review of the laboratory work on peroxyl radical reactions [*Lightfoot et al.*, 1992] indicates that the $CH_2O$ channel of the $HO_2 + CH_3O_2$ reaction has negligible yield at pressures above 50 torr. On the basis of the weight of the evidence, *Lightfoot et al.* [1992] conclude that the $HO_2 + CH_3O_2$ reaction produces exclusively $CH_3OOH$ and $O_2$ under tropospheric conditions.

[38] *Jaeglé et al.* [2000] observed that the best correlation between high levels of $CH_2O$ and other measured species in the SONEX campaign was with methanol. *Singh et al.* [2000] speculate that the heterogeneous conversion of methanol to $CH_2O$ on aerosols could occur. No measurements of $CH_3OH$ or aerosols were made on the P-3 during NARE 97. Using typical maritime aerosol sizes and number concentrations [*Whitby*, 1978], we calculate that the heterogeneous conversion of methanol would require methanol to have a reactive uptake coefficient $\approx 4 \times 10^{-3}$ in order to account for a 0.4 ppbv $d^{-1}$ source of $CH_2O$. *Jaeglé et al.* [2000] suggest an uptake coefficient of 0.01 for such a process. Given the uncertainties involved, the agreement between these estimates is reasonable. However, because aerosol number concentration and surface area generally decrease with altitude, one would expect a strong altitude dependence to such a mechanism, which does not seem apparent in the altitude-independent discrepancies found in NARE 97.

[39] Emission of $CH_2O$ and other carbonyl compounds by the ocean has been observed [*Zhou and Mopper*, 1997] and is not considered in our model. Other possible sources of $CH_2O$ not included in the model include the photochemistry of halogen radicals with methane [*DeMore et al.*, 1997]. Both of these possibilities, if they occurred in the NARE region, would tend to cause a greater discrepancy between model and measurements in the marine boundary layer than at higher altitudes, contrary to the fairly constant bias with altitude seen here.

[40] Another possibility is that there are additional formaldehyde precursors present in the remote troposphere which were not measured on the P-3 and therefore are not included as input to the model. *Weller et al.* [2000] suggested ethene and propene oxidation as a possible explanation for methane-only box model underestimates of measured [$CH_2O$] in the remote Atlantic. The NARE 97 measurements for our constant air mass legs indicated that ethene and propene levels were usually below the instrument detection limit of a few pptv. Furthermore, the altitude-independent model-measurement discrepancies found here point to $CH_2O$ precursors which are relatively long-lived (lifetimes of several days or more). Possible candidates include oxygenated VOCs such as organic peroxides, carbonyl compounds, and alcohols (besides methyl hydroperoxide, acetone, and methanol, which are already included in the model). Such compounds result from the oxidation of NMHCs and could persist in large enough concentrations to affect the formaldehyde budget, even though their NMHC precursors have already reacted away. It is difficult to estimate typical levels of oxygenates, in particular the larger molecular weight species, because they are generally not measured [*Singh et al.*, 1995]. We did include acetaldehyde and larger aldehydes (lumped as propanal) in our calculations and allowed them to reach photochemical steady state levels, but they did not contribute significant amounts of $CH_2O$. Additional VOCs with a total reactivity equivalent to 1.3 ppbv $CH_3OOH$, 12 ppbv acetone, or 11 ppbv $CH_3OH$ would bring the modeled [$CH_2O$] into agreement with the measurements. Measurements of total nonmethane organic carbon, $C_y$, from NARE 1993 at Chebogue Point, Nova Scotia, during the same season as NARE 97 [*Roberts et al.*, 1998] indicate typical $C_y$ levels of 10–20 ppb carbon (ppbC). Only a few ppbC of $C_y$ could be attributed to unmeasured VOCs in NARE 1993, but the uncertainties in the difference between $C_y$ and the measured speciated VOCs were on the order of 10 ppbC. Recent measurements [*O'Brien et al.*, 1997; *Pöschl et al.*, 2001] suggest levels of acetone in rural and remote continental locations of 1 ppbv or more, significantly higher than the concentrations used in this study, which were derived from correlations with CO observed in the remote marine troposphere and lowermost stratosphere [*Singh et al.*, 1995, 1997]. However, the true acetone levels in the NARE 97 background air masses are unlikely to be as high as the 12 ppbv needed to account for the $CH_2O$ discrepancy. *Lewis et al.* [2000] show that conventional chromatographic techniques probably substantially underestimate the levels of large molecular weight aromatic and oxygenated VOCs in urban air samples, but similar studies in more remote areas have not been carried out. We cannot rule out the possibility that VOCs which were not measured nor included in the model could represent the missing source of formaldehyde in NARE 97.

[41] The sensitivity of the model to uncertainties in the peroxide concentrations was also examined in more detail. We carried out an additional model run where, rather than being constrained by their measured values, [$CH_3OOH$] and [$H_2O_2$] were calculated to photochemical steady state simultaneously with the other species calculated in the base run. Under NARE 97 conditions, $CH_3OOH$ and $H_2O_2$ have photochemical lifetimes of about 1 and 2 days, respectively. Peroxides also rapidly deposit to the surface and can be uptaken by cloud droplets, so models that do not include these

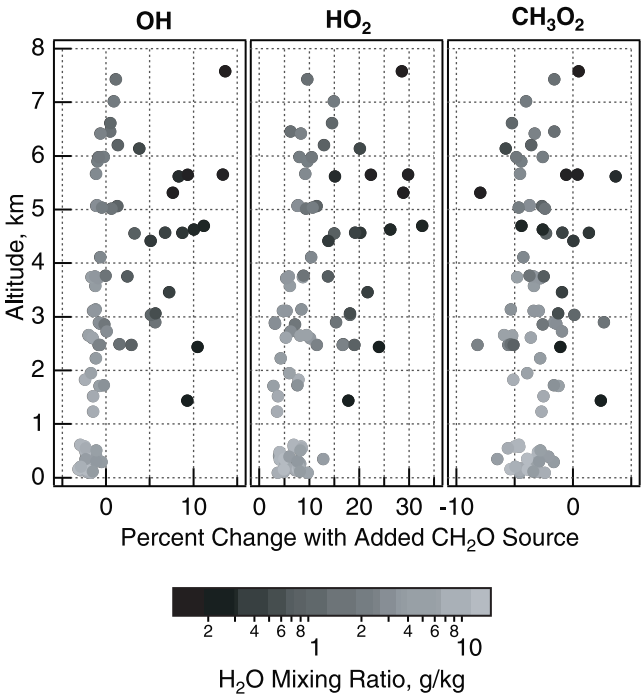


**Figure 10.** Effect of adding a 0.4 ppbv $d^{-1}$ source of $CH_2O$ on the levels of OH, $HO_2$, and $CH_3O_2$ as a function of altitude and $H_2O$ mixing ratio, compared with the base model run.

physical losses will tend to overestimate their concentrations. Indeed, we find that for the overall data set the model overestimates the measured peroxide concentrations by a factor of 2 or more. We restricted the data set to only those points which were in the free troposphere for at least the previous 3 days before measurement, to ensure that we could assume photochemical steady state in the peroxides as well as $CH_2O$. This highly restricted data set of 26 points omits the points which showed signs of recent transport (as discussed above) and all data below 2 km. Calculated [$CH_2O$] for this reduced data set is the same whether we constrained [$CH_3OOH$] and [$H_2O_2$] to measured values or calculated them to photochemical steady state: the median difference in model [$CH_2O$] between these two model approaches is 0.01 ± 0.01 ppbv (1σ) for these 26 points. NCAR [$CH_2O$] is greater than the model but within the uncertainties for these 26 points, with median differences of 0.08 ± 0.09 and 0.09 ± 0.09 ppbv (1σ) for the calculated and constrained peroxide approaches, respectively. Similarly, the median BNL-model [$CH_2O$] differences for these points are 0.13 ± 0.14 and 0.15 ± 0.14 ppbv. These model-measurement differences are similar to those seen in the full data set and when the data are broken down into altitude bins. On the other hand, modeled peroxide levels are in good agreement with measurements for these 26 points. Median measured [$CH_3OOH$] was 0.25 ppbv and [$H_2O_2$] = 0.41 ppbv, with reported 1σ total uncertainties of ±25%, or ±0.06 ppbv for [$CH_3OOH$] and ±0.10 ppbv for [$H_2O_2$]. Median modeled-measured differences for these 26 points were 0.06 ppbv for [$CH_3OOH$] and 0.08 ppbv for [$H_2O_2$], both of which can be accounted for by the measurement uncertainty alone. These results imply that differences between calculated and measured [$CH_2O$] do not stem from an inaccurate measurement of [$CH_3OOH$] or [$H_2O_2$].

[42] Whatever the missing source may be, we can investigate the implications of model-measured $CH_2O$ discrepancies on radical species. We reran our model calculations including an additional 0.4 ppbv $d^{-1}$ source of $CH_2O$ at every point and examined the percent change in OH, $HO_2$, and $CH_3O_2$ levels compared with the base model run. Figure 10 shows the results of this comparison for 0–8 km as a function of $H_2O$ vapor mixing ratio. [OH] and [$HO_2$] show similar responses to the additional $CH_2O$. For the wetter air masses ($H_2O$ > 1 g $kg^{-1}$), [OH] and [$HO_2$] exhibit modest effects from increased formaldehyde, with [OH] changing by ±5% and [$HO_2$] increasing by up to 20%. In drier air, [OH] increases by as much as 15%, and [$HO_2$] increases by as much as 35%. This response reflects the fact that $CH_2O$ can be a significant source of $HO_2$ in wetter free tropospheric air but that $O_3$ photolysis followed by reaction of $O(^1D)$ with $H_2O$ is the dominant radical source. In drier air, however, the importance of formaldehyde as a radical source increases drastically. Regardless of humidity level, [$CH_3O_2$] generally shows a decrease of a few percent with the added $CH_2O$ source, resulting from increases in [$HO_2$] increasing the rate of the $HO_2$ + $CH_3O_2$ reaction. Underestimating [$CH_2O$] in drier air will lead to a significant underestimate of total radical levels, leading to overestimates of NMHC lifetimes and underestimates of $O_3$ production rates for these conditions. The significance of a [$CH_2O$] underestimate will grow at higher altitudes, which are increasingly drier and where $CH_2O$ becomes one of the dominant sources of radicals. Hence we conclude that a correct calculation of tropospheric $CH_2O$ levels is indeed crucial.

## 4. Conclusion

[43] Measurements of formaldehyde by two independent instruments over the midlatitude North Atlantic Ocean from 0 to 8 km were compared to a box model. The model is constrained by the concentrations of NMHCs and $CH_3OOH$ measured coincidentally with $CH_2O$ and by methane, acetone, and methanol concentrations taken from other studies. Selection of air masses by their chemical constituents and calculated histories appears to indicate that the considered data set was representative of the unpolluted North Atlantic troposphere. The calculated source terms confirm this assessment, showing that nearly all the formaldehyde in these air masses should have been produced from methane oxidation. However, while the differences between the two $CH_2O$ instruments are somewhat larger than expected, there is a systematic underprediction by the model, and the median measured [$CH_2O$] is a factor of 2 larger than calculated. An analysis of the model uncertainties indicates that no single model input parameter could be responsible for such a discrepancy if the stated uncertainties for these parameters are correct. We conclude that the model-measurement differences are not due to some fundamental error in the methane oxidation scheme. A consideration of the possible reasons for the model underprediction of $CH_2O$ indicates that the error most likely is in the model source terms. We suggest one possible source of the model underestimate is its failure to account for unmeasured formaldehyde precursor species such as oxygenated VOCs.

[44] This study points out a number of improvements that could be made in future investigations of formaldehyde. Instrument precision is still an issue for both techniques used in this study, particularly in an aircraft implementation. In order to reduce the model [$CH_2O$] uncertainty, more laboratory determinations of various reaction rate coefficients (in particular that of $HO_2$ + $CH_3O_2$) and photolysis parameters are needed to reduce their uncertainty limits. Most importantly, more field campaigns such as NARE 97 which probe remote portions of the troposphere are needed. These field experiments should include coincident measurements of OH and peroxyl radicals and of the VOCs known to produce formaldehyde. In particular, we suggest the inclusion of instruments for detecting often unmeasured VOCs, such as aldehydes, ketones, alcohols, and other oxygenates.

[45] **Acknowledgments.** The authors wish to thank D. D. Parrish for the use of his data, his close reading of the manuscript, and his helpful comments. M. J. Evans is grateful for the efforts and financing of the British Atmospheric Data Centre, the UK Met Office, the UK Universities Global

Atmospheric Modeling Programme, and the UK Natural Environment Research Council. ACSOE publication ACP059.

## References

Arlander, D. W., D. R. Cronn, J. C. Farmer, F. A. Menzia, and H. H. Westberg, Gaseous oxygenated hydrocarbons in the remote marine troposphere, *J. Geophys. Res.*, *95*, 16,391–16,403, 1990.

Arlander, D. W., D. Brüning, U. Schmidt, and D. H. Ehhalt, The tropospheric distribution of formaldehyde during TROPOZ II, *J. Atmos. Chem.*, *22*, 251–268, 1995.

Atkinson, R., Gas-phase tropospheric chemistry of organic compounds, *J. Phys. Chem. Ref. Data Monogr.*, *2*, 1994.

Ayers, G. P., R. W. Gillett, H. Granek, C. de Serves, and R. A. Cox, Formaldehyde production in clean marine air, *Geophys. Res. Lett.*, *24*, 401–404, 1997.

Brasseur, G. P., D. A. Hauglustaine, and S. Walters, Chemical compounds in the remote Pacific troposphere: Comparison between MLOPEX measurements and chemical transport model calculations, *J. Geophys. Res.*, *101*, 14,795–14,813, 1996.

Dahlback, A., and K. Stamnes, A new spherical model for computing the radiation field available for photolysis and heating at twilight, *Planet. Space Sci.*, *39*, 671–683, 1991.

DeMore, W. B., S. P. Sander, D. M. Golden, R. F. Hampson, M. J. Kurylo, C. J. Howard, A. R. Ravishankara, C. E. Kolb, and M. J. Molina, Chemical kinetics and photochemical data for use in stratospheric modeling, Evaluation number 12, *JPL Publ.*, *97-4*, 1997.

Dlugokencky, E. J., L. P. Steele, P. M. Lang, and K. A. Masarie, The growth rate and distribution of atmospheric methane, *J. Geophys. Res.*, *99*, 17,021–17,043, 1994.

Dunker, A. M., The decoupled direct method for calculating sensitivity coefficients in chemical kinetics, *J. Chem. Phys.*, *81*, 2385–2393, 1984.

Elterman, L., UV, visible and IR attenuation for altitudes to 50 km, *Rep. AFCRL-68-0153*, U.S. Air Force, Bedford, Mass., 1968.

European Centre for Medium-Range Weather Forecasts (ECMWF), The description of the ECMWF/WCRP level III global atmospheric data archive, Reading, UK, 1995.

Fried, A., Y.-N. Lee, G. Frost, B. Wert, B. Henry, J. R. Drummond, G. Hübler, and T. Jobson, Airborne $CH_2O$ measurements over the North Atlantic during the 1997 NARE campaign: Instrument comparisons and distributions, *J. Geophys. Res.*, *107*(D4), 10.1029/2000JD000260, 2002.

Frost, G. J., et al., Photochemical ozone production in the rural southeastern United States during the 1990 Rural Oxidants in the Southern Environment (ROSE) program, *J. Geophys. Res.*, *103*, 22,491–22,508, 1998.

Frost, G. J., et al., Photochemical modeling of OH levels during the Aerosol Characterization Experiment, *J. Geophys. Res.*, *104*, 16,041–16,052, 1999.

Harris, G. W., D. Klemp, T. Zenker, J. P. Burrows, and B. Mathieu, Tunable diode laser measurements of trace gases during the 1988 *Polarstern* cruise and intercomparisons with other methods, *J. Atmos. Chem.*, *15*, 315–326, 1992.

Heikes, B. G., Formaldehyde and hydroperoxides at Mauna Loa Observatory, *J. Geophys. Res.*, *97*, 18,001–18,013, 1992.

Heikes, B. G., et al., Formaldehyde methods comparison in the remote lower troposphere during the Mauna Loa Observatory Photochemistry Experiment 2, *J. Geophys. Res.*, *101*, 14,741–14,755, 1996.

Jacob, D. J., et al., Origin of ozone and $NO_x$ in the tropical troposphere: A photochemical analysis of aircraft observations over the South Atlantic basin, *J. Geophys. Res.*, *101*, 24,235–24,250, 1996.

Jaeglé, L., et al., Photochemistry of $HO_x$ in the upper troposphere at northern midlatitudes, *J. Geophys. Res.*, *105*, 3877–3892, 2000.

Lewis, A. C., N. Carslaw, P. J. Marriott, R. M. Kinghorn, P. Morrison, A. L. Lee, K. D. Bartle, and M. J. Pilling, A larger pool of ozone-forming carbon compounds in urban atmospheres, *Nature*, *405*, 778–781, 2000.

Lightfoot, P. D., R. A. Cox, J. N. Crowley, M. Destriau, G. D. Hayman, M. E. Jenkin, G. K. Moortgat, and F. Zabel, Organic peroxy radicals: Kinetics, spectroscopy, and tropospheric chemistry, *Atmos. Environ., Part A*, *26*, 1805–1961, 1992.

Liu, S. C., et al., A study of the photochemistry and ozone budget during the Mauna Loa Observatory Photochemistry Experiment, *J. Geophys. Res.*, *97*, 10,463–10,471, 1992.

Lowe, D. C., and U. Schmidt, Formaldehyde (HCHO) measurements in the nonurban atmosphere, *J. Geophys. Res.*, *88*, 10,844–10,858, 1983.

Mackay, G. I., D. R. Karecki, and H. I. Schiff, Tunable diode laser absorption measurements of $H_2O_2$ and HCHO during the Mauna Loa Observatory Photochemistry Experiment, *J. Geophys. Res.*, *101*, 14,721–14,728, 1996.

McKeen, S. A., et al., Photochemical modeling of hydroxyl and its relationship to other species during the Tropospheric OH Photochemistry Experiment, *J. Geophys. Res.*, *102*, 6467–6493, 1997.

Methven, J., Offline trajectories, calculation and accuracy, *UGAMP Tech. Rep. 44*, 22 pp., Dep. of Meteorol., Univ. of Reading, Reading, UK, 1997.

O'Brien, J. M., P. B. Shepson, Q. Wu, T. Biesenthal, J. W. Bottenheim, H. A. Wiebe, K. G. Anlauf, and P. Brickell, Production and distribution of organic nitrates, and their relationship to carbonyl compounds in an urban environment, *Atmos. Environ.*, *31*, 2059–2069, 1997.

Pöschl, U., et al., High acetone concentrations throughout the 0–12 km altitude range over the tropical rain forest in Surinam, *J. Atmos. Chem.*, *38*, 115–132, 2001.

Roberts, J. M., S. B. Bertman, T. Jobson, H. Niki, and R. Tanner, Measurement of total nonmethane organic carbon ($C_y$): Development and application at Chebogue Point, Nova Scotia, during the 1993 North Atlantic Regional Experiment campaign, *J. Geophys. Res.*, *103*, 13,581–13,592, 1998.

Singh, H. B., M. Kanakidou, P. J. Crutzen, and D. J. Jacob, High concentrations and photochemical fate of oxygenated hydrocarbons in the global troposphere, *Nature*, *378*, 50–54, 1995.

Singh, H. B., et al., Trace chemical measurements from the northern midlatitude lowermost stratosphere in early spring: Distributions, correlations, and fate, *Geophys. Res. Lett.*, *24*, 127–131, 1997.

Singh, H. B., et al., Distribution and fate of select oxygenated organic species in the troposphere and lower stratosphere over the Atlantic, *J. Geophys. Res.*, *105*, 3795–3805, 2000.

Stohl, A., M. Hittenberger, and G. Wotawa, Validation of the Lagrangian particle dispersion model FLEXPART against large scale tracer experiment data, *Atmos. Environ.*, *24*, 4245–4264, 1998.

Stohl, A., M. Trainer, T. Ryerson, J. Holloway, and D. Parrish, Export of $NO_y$ from the North American boundary layer during NARE 96 and NARE 97, *J. Geophys. Res.*, *107*, 10.1029/2001JD000519, in press, 2002.

Thompson, A. M., and O. C. Zafiriou, Air-sea fluxes of transient atmospheric species, *J. Geophys. Res.*, *88*, 6696–6708, 1983.

U.S. Standard Atmosphere, *Rep. NOAA-S/T 76-1562*, Natl. Oceanic and Atmos. Admin., Washington, D. C., 1976.

Weller, R., O. Schrems, A. Boddenberg, S. Gäb, and M. Gautrois, Meridional distribution of hydroperoxides and formaldehyde in the marine boundary layer of the Atlantic (48°N–35°S) measured during the Albatross campaign, *J. Geophys. Res.*, *105*, 14,401–14,412, 2000.

Whitby, K. T., The physical characteristics of sulfur aerosols, *Atmos. Environ.*, *12*, 135–159, 1978.

Zafiriou, O. C., J. Alford, M. Herrera, E. T. Peltzer, R. B. Gagosian, and S. C. Liu, Formaldehyde in remote marine air and rain: Flux measurements and estimates, *Geophys. Res. Lett.*, *7*, 341–344, 1980.

Zhou, X., and K. Mopper, Photochemical production of low molecular weight carbonyl compounds in seawater and surface microlayer and their air-sea exchange, *Mar. Chem.*, *56*, 201–213, 1997.

Zhou, X., Y.-N. Lee, L. Newman, X. Chen, and K. Mopper, Tropospheric formaldehyde concentration at the Mauna Loa Observatory during the Mauna Loa Observatory Photochemistry Experiment 2, *J. Geophys. Res.*, *101*, 14,711–14,719, 1996.

J. R. Drummond, Department of Physics, University of Toronto, Toronto, Ontario, Canada M5S 1A1.

M. J. Evans, Department of Earth and Planetary Sciences, Harvard University, Cambridge, MA 02138, USA.

F. C. Fehsenfeld, G. J. Frost, P. D. Goldan, J. S. Holloway, G. Hübler, R. Jakoubek, W. C. Kuster, J. Roberts, T. B. Ryerson, D. T. Sueper, and M. Trainer, Aeronomy Laboratory, NOAA, Boulder, CO 80303, USA. (gfrost@al.noaa.gov)

A. Fried, B. Henry, C. Stroud, and B. Wert, Atmospheric Chemistry Division, NCAR, Boulder, CO 80305, USA.

B. T. Jobson, Battelle, Pacific Northwest National Laboratory, Richland, WA 99352, USA.

K. Knapp, Department of Chemistry, Pennsylvania State University, York Campus, York, PA 17403, USA.

Y.-N. Lee, Environmental Chemistry Division, Brookhaven National Laboratory, Upton, NY 11973, USA.

J. Rudolph, Centre for Atmospheric Chemistry, Department of Chemistry, York University, North York, Ontario, Canada M3J 1P3.

A. Stohl, Lehrstuhl für Bioklimatologie und Immissionsforschung, Technische Universität München, Freising-Weihenstephan, D-85354 Germany.

J. Williams, Abteilung Chemie der Atmosphare, Max Planck Institut für Chemie, D-55020 Mainz, Germany.